

A SYSTEM FOR SIMULTANEOUSLY DRIVING
THREE DISCRETE NUCLEAR RESONANCES IN GaAs:
THEORY AND EXPERIMENT

by

Daniel N. Jenson

A senior thesis submitted to the faculty of
Brigham Young University
in partial fulfillment of the requirements for the degree of

Bachelor of Science

Department of Physics and Astronomy

Brigham Young University

December 2008

Copyright © 2008 Daniel N. Jenson

All Rights Reserved

BRIGHAM YOUNG UNIVERSITY

DEPARTMENT APPROVAL

of a senior thesis submitted by

Daniel N. Jenson

This thesis has been reviewed by the research advisor, research coordinator,
and department chair and has been found to be satisfactory.

Date

John Colton, Advisor

Date

Eric Hintz, Research Coordinator

Date

Scott Sommerfeldt, Chair

ABSTRACT

A SYSTEM FOR SIMULTANEOUSLY DRIVING THREE DISCRETE NUCLEAR RESONANCES IN GaAs: THEORY AND EXPERIMENT

Daniel N. Jenson

Department of Physics and Astronomy

Bachelor of Science

Quantum computers will use quantum mechanical properties to perform certain tasks much faster than traditional computers. Realization of one quantum computing scheme requires a measurement of the T_2 electron spin lifetime in GaAs. Electron and nuclear interactions prevent an accurate measurement of T_2 by optically detected spin echo. Attempts to eliminate nuclear effects using NMR have been unsuccessful, probably due to insufficient magnetic field strength at one or more of the three resonant frequencies. Transmission line effects and mismatched impedances may have limited the current delivered to the NMR coil. Several impedance matching methods are considered, using computer models to account for transmission line effects and predict current delivered to the coil. Two methods are selected—both use three coils on the same circuit, each tuned to one of the resonant frequencies. Experiments show that neither method is a viable solution. It is recommended that further tests be performed with three coils on separate circuits, each tuned and driven around one of the resonant frequencies.

ACKNOWLEDGEMENTS

Funding for this research was provided by:

BYU OFFICE OF RESEARCH AND CREATIVE ACTIVITIES

BYU DEPARTMENT OF PHYSICS AND ASTRONOMY

Contents

Table of Contents	vii
1 Motivation	1
1.1 Quantum computing.....	1
1.2 Electron spin in GaAs.....	3
1.3 Nuclear resonance.....	4
2 Theory	7
2.1 Magnetic field from coil.....	7
2.2 Transmission line effects.....	10
2.3 Impedance matching.....	13
3 Experiment	17
3.1 Coil characterization.....	17
3.2 B-field measurements.....	19
3.3 Impedance matching results.....	22
3.4 Analysis and recommendation.....	26
Bibliography	29
A Unmatched transmission line model	31
B Matched transmission line model	35
C Three-coil model	41
Index	45

Chapter 1

Motivation

Electron spin in semiconductors is being studied for potential use in quantum computing.

A quantum computer will theoretically use quantum mechanical properties to perform certain operations much faster than standard computers. The bit which carries

information used in computing operations will be replaced by the quantum bit (qubit).

Electron spin could be used as a qubit if it can be shown to exhibit favorable properties.

The spin must be controllable, i.e. when an electron is placed in a certain spin state it will not randomly reorient itself before the computing operation is complete. Therefore it is necessary to characterize electron behavior before recommending a material for quantum computing.

1.1 Quantum computing

A classical computer of n bits can be in any one of 2^n possible states. In contrast, the state of a quantum computer of n qubits (quantum binary digits) is described by a quantum superposition of 2^n states each existing simultaneously. This important distinction is fundamental to quantum computing. Along with other quantum mechanical properties, it

provides an improved method for performing certain algorithms. Computer problems that require a “brute force” approach—guessing every possible answer until the correct one is found—could be solved by a quantum computer in a fraction of the time it would take a classical computer. Typical examples include fast database searching and factoring multiples of very large prime numbers [1].

Before being developed into a workable quantum computer, a system must first meet five basic requirements, articulated by David DiVincenzo of IBM. The following are paraphrased from DiVincenzo [1].

1. The system needs to have well-defined qubits, scalable in quantity. In other words, it must be possible to add qubits to the system similar to how classical computers can be upgraded with extra memory.
2. There must be a way to initialize the entire system to a basic state, such as setting all of the bits in a classical computer to zero.
3. Qubits must not decohere faster than operations can be performed on them.
4. There must be a system of quantum gates to operate on the qubits.
5. There must be a way to detect the state of the qubits.

Several different quantum computing architectures have been proposed to meet the above requirements. Candidates include superconducting systems [2], optical systems [3], NMR systems [4], and electron spin-based systems using diamonds [5] or quantum dots [6]. The present research is focused on electron spins in semiconductors, where electrons are confined similar to the quantum dot case. The goal is to positively or negatively confirm that a collection of spins remains coherent long enough to satisfy the third criteria for quantum computing.

1.2 Electron spin in GaAs

The amount of time an electron takes to reorient its spin is described by the electron spin-lifetime. There are three different measurements of spin-lifetime: T_1 , T_2 , and T_2^* [7]. T_1 is the time it takes for a spin to completely flip in the presence of an external magnetic field (without artificial stimulus). This requires a transfer of energy and is the longest spin-lifetime [8]. T_2 is called the transverse spin-lifetime and describes how long a group of electrons stay in a given spin-state regardless of an external magnetic field. T_2 is the quantity of interest in quantum computing. T_2^* is the shortest spin-lifetime, involving T_2 effects as well as additional dephasing caused by defects or inhomogeneities in the material [9].

A standard method of negating T_2^* dephasing to accurately measure the T_2 spin-lifetime is the spin-echo experiment. In the spin-echo sequence a microwave pulse is used to flip electron spins 90° in the transverse plane (perpendicular to external magnetic field). A longer pulse follows, causing a 180° rotation. During the time between pulses, spins will precess at different rates due to material defects and T_2 . After the second pulse, the precession due to defects will tend to realign the spins and any remaining decoherence is due to T_2 [10]. In order for a material to be useful in quantum computing, T_2 must be much longer than the time it takes to perform a single operation—on the order of a microsecond or longer [11].

For a spin-echo experiment to be performed an external magnetic field must be applied and one electron spin state must be preferentially occupied. The BYU spin dynamics laboratory has a liquid-He-cooled superconducting magnet—Oxford Instruments Spectromag®. The Spectromag® supplies the magnetic field (up to 7T) and

cools the sample (down to 1.5K) so that spins will tend to align parallel to the field. A unique sample holder has been designed for use inside the magnet. Rexolite®, a polystyrene microwave plastic, is used for the sample holder because it has very good dielectric properties. The sample holder sits in between very high dielectrics inside a conducting shell. The shell is fastened to the sample rod and placed inside the magnet. A coaxial cable running down the sample rod pumps microwaves into the shell, which resonates with specific microwave frequencies determined by the dielectric constant. This resonant cavity focuses enough microwave power on the sample to coherently flip electron spins as required in a spin-echo process.

T_2 has been successfully measured in several different structures. The material current being studied is GaAs, for which T_2 has not (to the author's knowledge) been measured. The specific sample being studied has been doped with extra electrons which extend the T_2 lifetime. Both theoretical analyses and measurements of T_1 suggest that T_2 may be long enough for this material to be a good candidate for quantum computing [7]. One of the greatest obstacles to obtaining the measurement is the mutual interaction of nuclear and electron spins.

1.3 Nuclear resonance

The strong coupling of nuclear and electron spins in GaAs prevents an accurate measurement of T_2 [7]. Whenever electrons are aligned the resulting fields affect the nuclei, which in turn produce fields affecting the electron arrangement. In order to isolate the electrons, the nuclear spin effects must be neutralized. One way to accomplish that is to cause the nuclear spins to continually flip direction so a collection of spins is, on

average, pointing neither up nor down. An alternating magnetic field at the nuclear resonant frequencies should produce the desired effect. So while microwaves in the resonant cavity are used to manipulate the electrons, another system is required to control the nuclei.

A split solenoid, similar to a rectangular Helmholtz coil, is used to apply a magnetic field to the sample. The coil is constructed of 30 gauge insulated copper wire (AWG) wrapped around the sample holder before the sample is placed in the resonant cavity. When the sample is placed in the cavity, the coil leads are fed through a hole in the cavity and connected to a transmission line (parallel wire or coaxial cable) extending down the sample rod. Current to the coil is supplied by a Tektronix function generator via an rf amplifier from Amplifier Research.

To resonate the nuclei the alternating current through the coil must be at the resonant frequency of each nucleus. The sample contains one arsenic and two gallium isotopes which each have distinct resonant frequencies at roughly 9, 14, and 19 MHz [12]. The initial method used to obtain resonance was to set the function generator to sweep from 5 MHz to 25 MHz with constant amplitude at a rate of 1 kHz. Assuming that the function generator hits every frequency in the sweep range, each nucleus should be resonated once every 1 ms. However, initial attempts to measure T_2 using this method of NMR were unsuccessful, likely due to incomplete or insufficient nuclear resonance. A better understanding of the circuit electrodynamic at relevant frequencies is required to identify the cause of failure and design a working system.

Chapter 2

Theory

There are at least two probable reasons that previous attempts at NMR were unsuccessful. Either the function generator skips over one or more of the resonant frequencies or the current through the coil is not producing a strong enough magnetic field to manipulate the nuclei. Spectrum analysis of the function generator output indicates that none of the frequencies are being skipped. Therefore, it seems likely that the magnetic field is not strong enough. If magnetic field strength is the limiting factor then increasing current getting to the coil at the resonant frequencies will solve the NMR problem.

2.1 Magnetic field from coil

Magnetic field strength inside the coil is directly proportional to current through the coil at a given moment. Making the assumption that instantaneous current magnitude is uniform throughout the coil and exploiting the coil's convenient rectangular shape, the magnetic field at the center can be solved with the law of Biot-Savart. The closely spaced loops are approximated by a single loop on each side with current nI , where n is the number of loops in one side of the coil and I is the current through a single wire at any

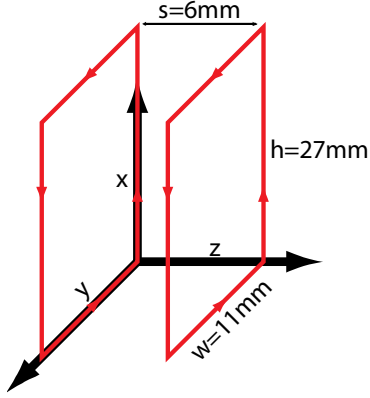


Figure 2.1 Dimensions and layout of coil model used to calculate magnetic field (not to scale)

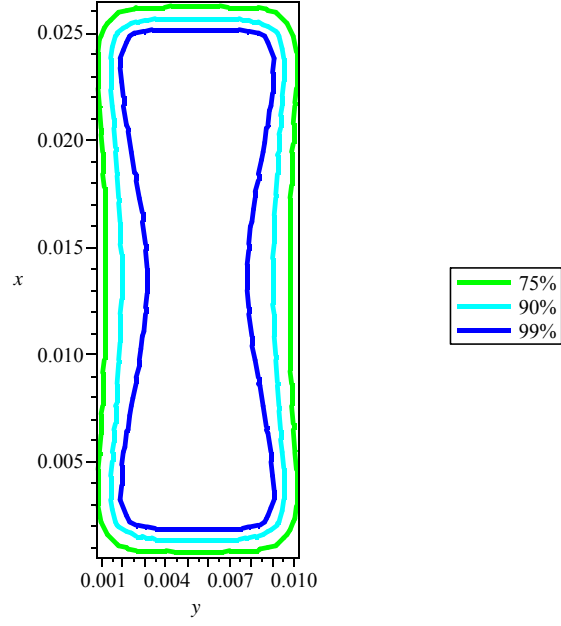


Figure 2.2 Magnetic field strength intersecting the $z = s/2$ plane as a percentage of field strength at the center

point in the coil. Each side of the coil can be treated as a separate contribution to the magnetic field as follows:

$$\mathbf{B}(\mathbf{r}') = \sum_{i=1}^8 \mathbf{B}_i(\mathbf{r}'), \quad (1)$$

where each contribution is given by:

$$\mathbf{B}_i(\mathbf{r}') = \frac{\mu_0 n I}{4 \pi} \int \frac{(d\mathbf{l}_i \times (\mathbf{r}' - \mathbf{r}_i))}{|\mathbf{r}' - \mathbf{r}_i|^3}. \quad (2)$$

The first four pieces, corresponding to the coil half placed in the $z = 0$ plane (refer to Figure 2.1), are expanded below.

$$\mathbf{B}_1(\mathbf{r}') = \mathbf{B}_1(x', y', z') = \frac{\mu_0 n I}{4 \pi} \int_0^h \left(- \frac{z'}{((x' - x)^2 + y'^2 + z'^2)^{3/2}} \hat{\mathbf{y}} + \frac{y'}{((x' - x)^2 + y'^2 + z'^2)^{3/2}} \hat{\mathbf{z}} \right) dx \quad (3)$$

$$\mathbf{B}_2(\mathbf{r}') = \mathbf{B}_2(x', y', z') = \frac{\mu_0 n I}{4 \pi} \int_0^h \left(\frac{z'}{\left((x'-x)^2 + (y'-w)^2 + z'^2 \right)^{3/2}} \hat{\mathbf{y}} - \frac{y'-w}{\left((x'-x)^2 + (y'-w)^2 + z'^2 \right)^{3/2}} \hat{\mathbf{z}} \right) dx \quad (4)$$

$$\mathbf{B}_3(\mathbf{r}') = \mathbf{B}_3(x', y', z') = \frac{\mu_0 n I}{4 \pi} \int_0^w \left(-\frac{z'}{\left(x'^2 + (y'-y)^2 + z'^2 \right)^{3/2}} \hat{\mathbf{x}} + \frac{x'}{\left(x'^2 + (y'-y)^2 + z'^2 \right)^{3/2}} \hat{\mathbf{z}} \right) dy \quad (5)$$

$$\mathbf{B}_4(\mathbf{r}') = \mathbf{B}_4(x', y', z') = \frac{\mu_0 n I}{4 \pi} \int_0^w \left(\frac{z'}{\left((x'-h)^2 + (y'-y)^2 + z'^2 \right)^{3/2}} \hat{\mathbf{x}} - \frac{x'-h}{\left((x'-h)^2 + (y'-y)^2 + z'^2 \right)^{3/2}} \hat{\mathbf{z}} \right) dy \quad (6)$$

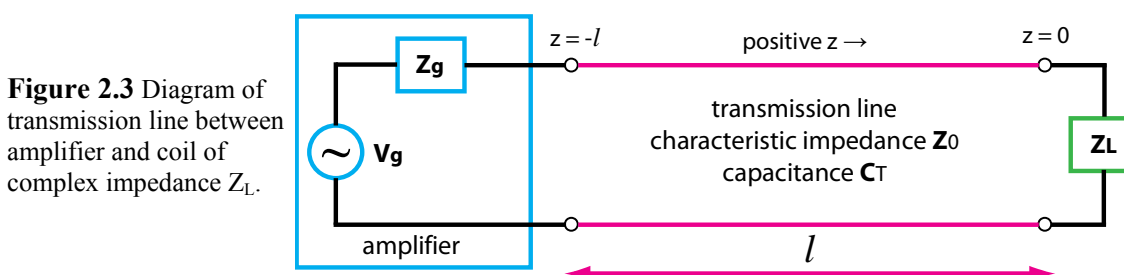
The other four pieces can be obtained by substituting $(z' - s)$ in place of every z' on the right hand side of Eqs. 3-6. Clearly an analytic solution would be far too complicated to be useful, but since only the field at the sample is important, the calculation can be simplified to find the field at the center. Figure 2.2 shows the relative uniformity of the field intersecting the $z = s/2$ plane. At the center any contributions to the field in the $\hat{\mathbf{x}}$ or $\hat{\mathbf{y}}$ directions will cancel out and the contribution in the $\hat{\mathbf{z}}$ direction will be the same from each half of the coil. The solution then reduces to:

$$\mathbf{B}_{\text{center}} = \frac{\mu_0 n I}{2 \pi} \hat{\mathbf{z}} \left(\int_0^h \frac{w}{\left(\left(\frac{1}{2} h - x \right)^2 + \frac{1}{4} w^2 + \frac{1}{4} s^2 \right)^{3/2}} dx + \int_0^w \frac{h}{\left(\frac{1}{4} h^2 + \left(\frac{1}{2} w - y \right)^2 + \frac{1}{4} s^2 \right)^{3/2}} dy \right). \quad (7)$$

Eq. 7 with the coil dimensions shown in Figure 2.1 predicts a center field strength of 1.23 Gauss per nI , with I in Amperes. A field strength of about $\frac{1}{2}$ Gauss was sufficient for a similar experiment [12]. A coil with five turns on each side would need to receive about 80 mA of current to produce that field. More is desirable.

2.2 Transmission line effects

Ohm's law for alternating current is written $V = IZ$, where V , I , and Z are the complex voltage, current, and impedance, respectively. Unfortunately, Ohm's law alone is insufficient when the length of electrical line is large compared with the wavelength of the electromagnetic wave on the line at the signal frequency. When the line length exceeds $1/10$ of the wavelength (a somewhat arbitrary number) then the approximation of constant voltage along a conducting wire is no longer valid. Furthermore, when an electromagnetic wave travels from one medium into another medium only part of the energy from the incident wave is transmitted and some is reflected. This familiar principle from optics is equally pertinent to electrostatics. A reflected wave interferes with the incident wave and can set up a standing wave on the line with nodes that experience zero voltage. The fraction of energy reflected and the shape of the standing wave are both functions of wavelength (and consequently frequency).



The reflection coefficient Γ for a signal going from a transmission line into a load is written as:

$$\Gamma = \frac{Z_L - Z_0}{Z_L + Z_0}. \quad (8)$$

where Z_L is the complex impedance of the load and Z_0 is the characteristic impedance of the transmission line. Refer to Figure 2.3. Characteristic impedance varies with frequency, but for low frequencies (below 100 MHz) it can generally be treated as a constant. The voltage at a point z from the end of the transmission line (by convention, the positive direction is defined to be from the source to the load) is given by:

$$V(z) = V^+ (e^{-i\beta z} + \Gamma e^{i\beta z}), \quad (9)$$

where V^+ is the voltage of the forward moving wave and β is equal to $\omega Z_0 C_T$, ω being the usual angular frequency and C_T the capacitance of the transmission line. To solve for V^+ , Eq. 9 is evaluated at the beginning of the transmission line ($z = -l$) where the transmission line is connected to the amplifier. The result is:

$$V^+ = \frac{\frac{V_g Z_{in}}{Z_g + Z_{in}}}{e^{i\beta l} + \Gamma e^{-i\beta l}}. \quad (10)$$

The numerator in Eq. 10 is the output voltage of the amplifier from a simple application of Ohm's Law where V_g and Z_g are the amplifier voltage and output impedance, respectively, and Z_{in} is the effective impedance seen by the amplifier looking into the transmission line, obtained from the "transmission line equation":

$$Z_{in} = \frac{Z_0 (Z_L + i Z_0 \tan(\beta l))}{Z_0 + i Z_L \tan(\beta l)}. \quad (11)$$

Eqs. 8-11 provide all the mathematics needed to find the voltage at the end of the transmission line ($z = 0$), provided that amplifier, coil, and transmission line characteristics are known. For a more detailed discussion of transmission line effects and calculations see Pozar's Microwave Engineering [13].

A computer model was used to predict current through the coil as a function of signal frequency, taking transmission line effects into account. See Appendix A for complete MATLAB code. Figure 2.4 shows the results with two different load conditions, given in Table 2.1. Evidently the current delivered to the coil is quite sensitive to coil resistance and inductance as well as signal frequency.

	Resistance (Ω)	Inductance (μH)	Description
Coil 1	$0.916 + 7.46559 \cdot 10^{-6}f$	15	Estimated values for a coil used in a previous run of experiments
Coil 2	$0.38 + 7.65 \cdot 10^{-7}f$	1.2	Values measured using LCR meter as described in Section 3.1

Table 2.1 Coil characteristics used to produce the current models in Figure 2.3. In addition to the values listed, both models used transmission line values from the manufacturers data sheet for the coaxial cable used in the most recent run of experiments: $Z_0 = 40\Omega$, $l = 1.5\text{m}$, $C_T = 174\text{pF}$.

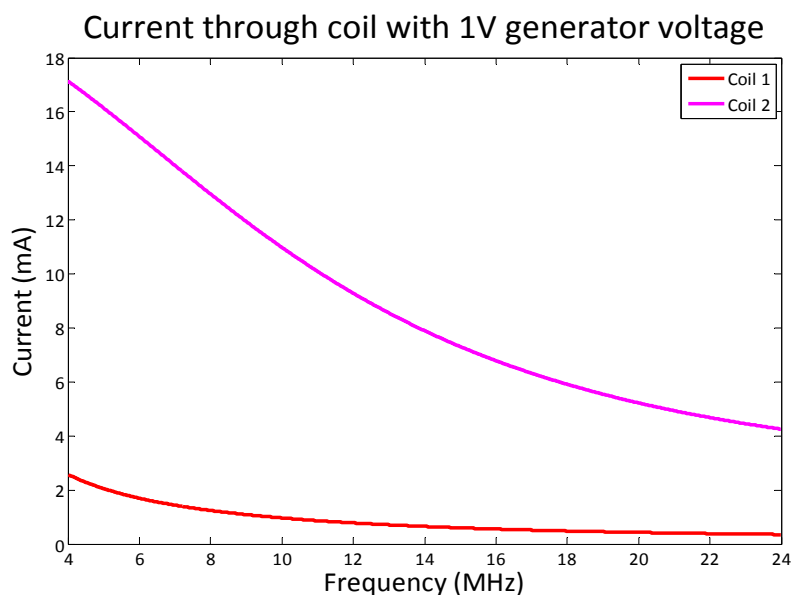


Figure 2.4 Model of current through coil at the end of a coaxial cable transmission line using values listed in Table 2.1.

2.3 Impedance matching

As shown in Figure 2.4 and Table 2.1, higher current is obtained at lower frequencies and lower values of coil inductance. Lower inductance is obtained from fewer turns in the coil. A five-turn coil (coil 2 in Table 2.1) will be used in subsequent models and experiments. The apparent frequency dependence is more appropriately described as wavelength dependence. The lower current at higher frequencies is a result of shorter wavelength along the transmission line—transmission line effects become more pronounced. A different type of transmission line with a lower dielectric constant would have longer wavelengths at the same frequencies. Two parallel wires without any insulating material in between should increase the signal wavelength to nearly the vacuum wavelength. For this reason, all models and experiments from this point on are done using parallel wires.

Theoretically, amplifier voltage could be increased until current through the coil is sufficient to produce the required magnetic field. In reality, however, the amplifier has a maximum power output. Additionally, even if the amplifier could handle the power requirement a significant amount of power from off-resonant frequencies would be wasted, contributing to heat at the sample. A more refined approach is to modify the circuit so that natural resonances will occur at the desired frequencies. This type of approach, called impedance matching, is typically used to match a single frequency or a small range of frequencies to the amplifier output impedance. For maximum effectiveness, a matching circuit should be placed between the coil and the transmission line. In the present experiment, space constraints prevent a matching circuit between

transmission line and coil; modifications must instead be placed between the amplifier and transmission line to match Z_g and Z_{in} .

Several different options for impedance matching have been considered. A single series capacitor or inductor, determined by the behavior of Z_{in} at relevant frequencies, may serve to cancel reactance (Method A). Alternatively, Pozar describes a technique called “L-section” which uses two reactive elements—one in series and one in parallel—to match both reactance and resistance (Method B) [14]. Both of these methods can only match a single frequency, however. An innovative solution is to match three frequencies at once using three coils wrapped concentrically, each matched to a different frequency using one of the methods above. The separate transmission lines can then be attached in parallel before connecting to the amplifier. When the signal frequency matches one of the three parallel lines, most of the power will be drawn into that line. At unmatched frequencies most of the power will be reflected back to the amplifier.

Current models indicate that the three-coil solution may be the most effective. Figure 2.5 compares the three-coil solution using either Method A or Method B for impedance matching. Both methods provide some improvement over unmatched coils. Based on the computer model, Method A seems superior. However, recognizing that there may be errors or (almost certainly) oversimplifications in the models, both methods have been tested experimentally.

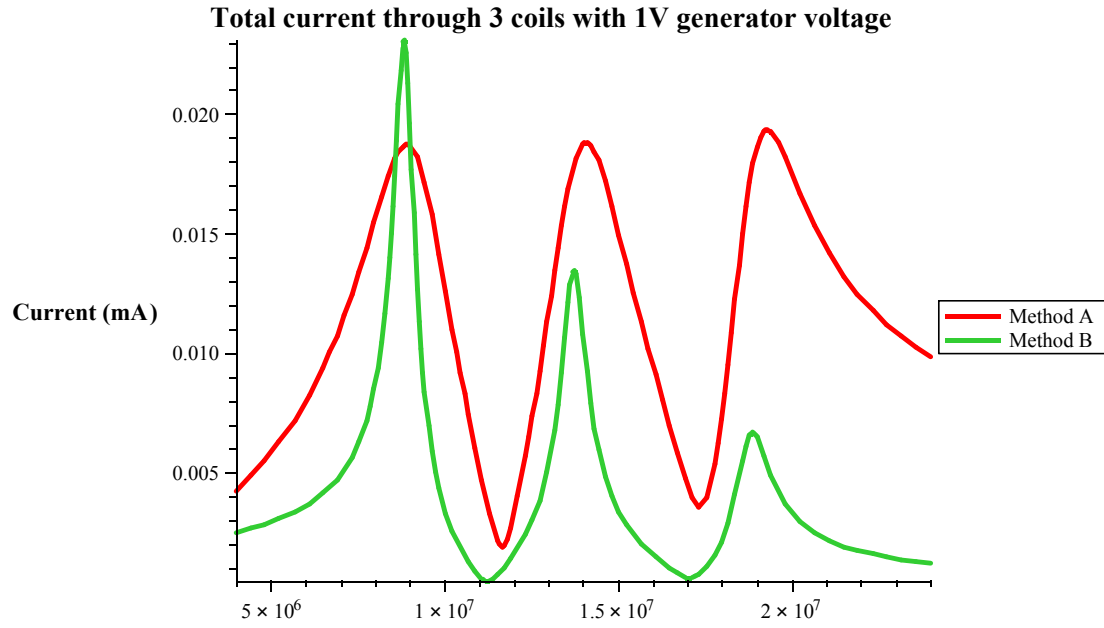


Figure 2.5 Model of total current through three coils, each at the end of a parallel wire transmission line. Method A uses a single capacitor on each line to cancel the reactance of the line at one of the matching frequencies. Method B uses L-section matching.

Chapter 3

Experiment

Three tightly wrapped coils, each with 5 turns per side, was used to test the two methods of impedance matching. The same gauge wire used for the coils was used for parallel wire transmission lines. Although GaAs experiments are performed at low temperatures inside the magnet bore, logistics prevent coil measurements while the cavity is inside the magnet. Instead, the sample rod was removed so that tests could be performed outside the magnet. If either impedance matching method is proven effective then it may be adapted to work with the slightly different conditions of the actual experiment.

3.1 Coil Characterization

Before a matching circuit could be built it was necessary to characterize the load impedance required in Eqs. 8 & 11. Attempts to estimate inductance from coil geometry were unsuccessful. DC measurements of coil resistance were likewise useless since skin effects and other AC phenomena create frequency dependence. Coil impedance values were obtained using an LCR meter (HP 4275A Multi-Frequency LCR Meter). The instrument measures the impedance magnitude $|Z|$ and phase angle θ at 10 distinct

frequencies between 10 kHz and 10 MHz. Resistance and reactance are then the real and imaginary parts of Z , respectively. Although the frequency range of the LCR meter is not high enough to reach all of the nuclear resonant frequencies, the data was extrapolated to higher frequencies.

The leads for a single coil were connected to the high and low test leads on the LCR meter. The two unused coils were left open-circuited to prevent induced current. Ten data points were taken for each coil before the sample holder was placed inside the resonant cavity. The procedure was then repeated with the coils inside the resonant cavity. As expected, enclosing the coils in a conducting shell significantly changed their impedances. The measurements inside the shell were used. Agreement between the three (nearly-identical) coils was satisfactory. The average values at each frequency are plotted in Figure 3.1, along with a curve fit from which expressions for resistance and reactance may be read.

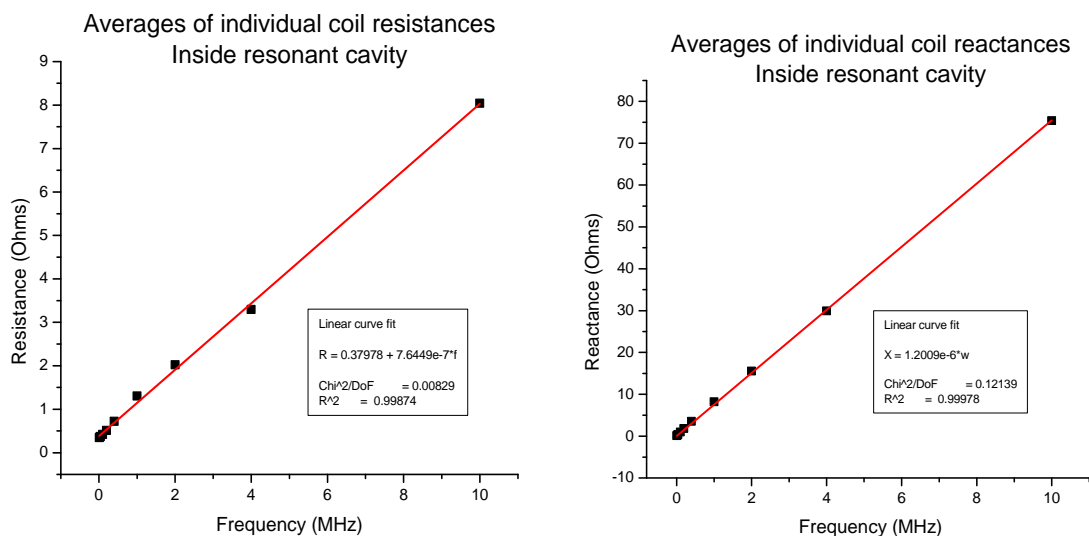


Figure 3.1 Coil data from LCR meter containing average values of individual coil measurements and curve fits.

The linear shape of the reactance curve is no surprise since the coils should be almost purely inductive. The inductance is simply the slope of the line. The resistance curve, on the other hand, is unexpectedly linear. No model has been found to adequately explain its shape. The DC resistance predicted by the curve fit is in agreement with measurement, however. At higher frequencies it is doubtful that the linearity persists, but at 24 MHz the predicted resistance is about 19Ω , which is not entirely unbelievable. For lack of a better method to measure resistance at higher frequencies, the expression for R in Figure 3.1 will have to suffice.

In coil characterization and in computer models in the previous chapter, the interaction between coils has been ignored. Mutual inductance will certainly have some influence on the total current and hence the magnetic field produced. The extent and outcome of that interaction is unknown, however. Only by actually measuring the magnetic field produced by the three-coil ensemble can the success (or failure) of impedance matching methods be known.

3.2 B-field Measurements

The EMF induced by a changing magnetic field can be viewed on an oscilloscope using a small pickup loop. Two different loops will be used. A 3 mm diameter loop is used to measure the field near the center. Another loop is made by wrapping a single turn coil around one side of the sample holder (at $z=0$, refer to Figure 2.1). This larger pickup loop is used to get a stronger and more reproducible signal than the small pickup loop. It will measure the average field through one side of the three-coil setup. Values measured by

the large pickup loop will be greater than those at the center, but frequency dependence should be the same for each.

Finding the magnetic field from the induced EMF is quite simple, but requires a few assumptions that may or may not be valid. The first assumption is that the magnetic field through either pickup loop takes the form,

$$\mathbf{B}(\omega, t) = B_0 \sin(\omega t) \hat{\mathbf{z}}. \quad (12)$$

Then assuming that the pickup loop is placed perfectly perpendicular to the field, the EMF can be written as,

$$\text{EMF} = -\frac{\partial \Phi}{\partial t} = -\frac{\partial}{\partial t} (\mathbf{B} \cdot \mathbf{A}) = -B_0 A \omega \cos(\omega t), \quad (13)$$

where A is the area enclosed by the pickup loop. The peak magnetic field can then be expressed as,

$$B_{\text{peak}} = \frac{\text{EMF}_{\text{peak}}}{\omega A}. \quad (14)$$

In the case of a non-uniform magnetic field, the right hand side of Eq. 14 gives the average peak magnetic field through the area.

To get the most accurate reading possible, the length of wire from the pickup loop to the oscilloscope is kept as short as possible. The small pickup loop is at the end of a 40 cm coaxial cable. The large pickup loop is connected to the oscilloscope by 25 cm parallel wires. Longer transmission lines leading to the pickup loops would create resonant frequencies within the sweep range, unrelated to the coil resonances. The short line length will ensure that any pickup loop resonances are well above the sweep range.

Initial measurements of magnetic field from a single coil on an unmatched coaxial cable transmission line revealed an unexpected phenomenon. At low power output

(below 500 mV peak to peak signal with the amplifier set at 50%) the signal through the small pickup loop placed near the center of the coil maintained a sinusoidal oscillation. At higher power, however, the oscillatory behavior changed dramatically. The overall signal frequency was still present, but higher order oscillations appeared. These additional frequency components have no clear relation to the signal frequency, as demonstrated in Figure 3.2. Whether these extra oscillations are due to some cavity resonance, amplifier mechanics, or transmission line effects, is not known. However, since they only appear at high power, Eq. 14 can still be used at low power.

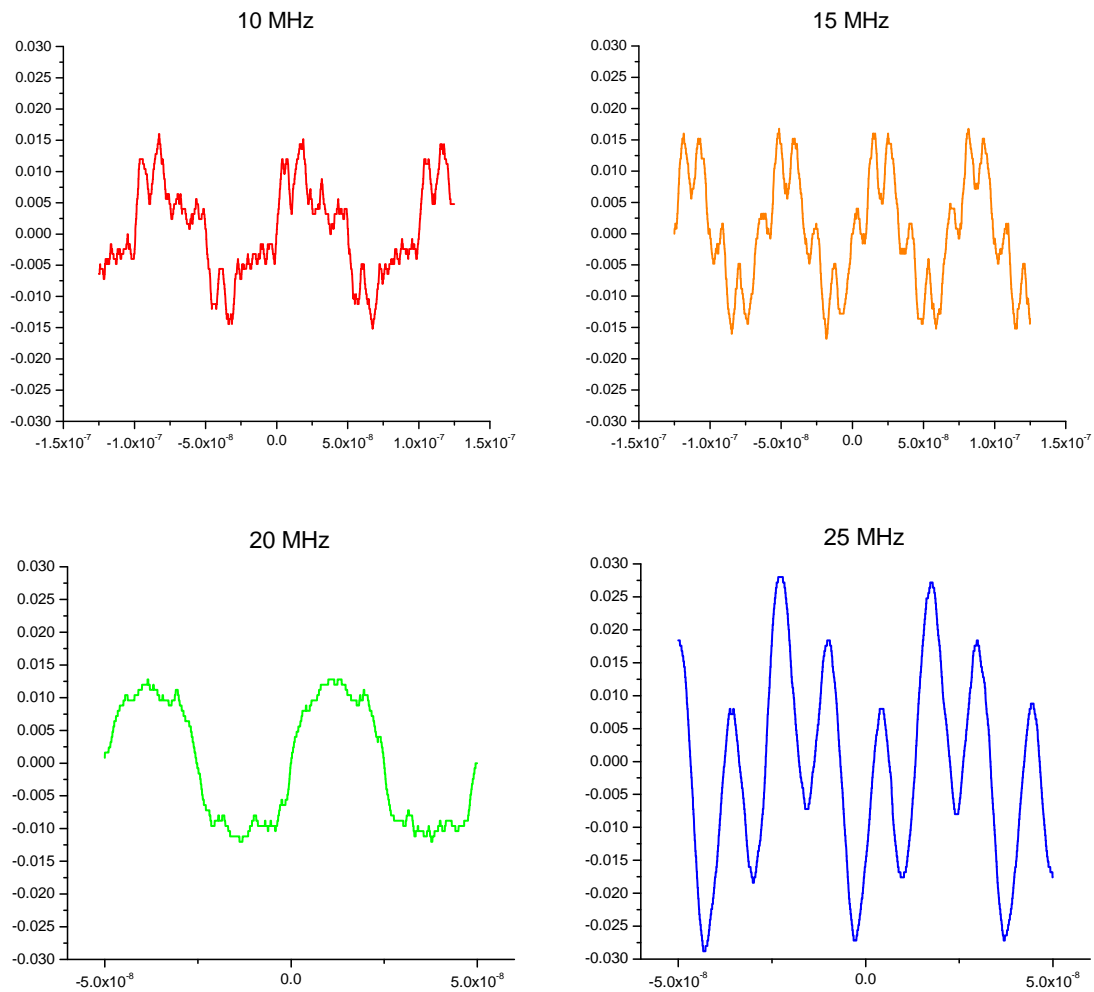


Figure 3.2 Voltage induced in the small pickup loop as a function of time for four different input frequencies.

3.3 Impedance matching results

Coil data obtained in section 3.1 allows a matching circuit to be constructed. Capacitance and inductance for the parallel wire transmission line are estimated from formulas given in Pozar [13]. The computer code in Appendix B finds which components will be needed for both single-element matching and L-section matching (Methods A and B, respectively). As it turns out, only capacitors are required. This is a convenient result, since variable capacitors are much cheaper than variable inductors. Furthermore, the size of capacitors required ranges from 16 pF to 760 pF—all reasonable values. If coaxial cable had been used rather than parallel wires, building the circuit would have been much trickier, involving very small inductors.

For Method A, three parallel-plate variable capacitors were placed between the amplifier and the transmission lines as shown in Figure 3.3. Method B used six variable capacitors and two non-variable capacitors configured as shown in Figure 3.4. These were both tested on parallel wires running through the sample rod and then again on parallel wires outside the sample rod. The magnetic field produced by the three-coil system was measured using both pickup loops.

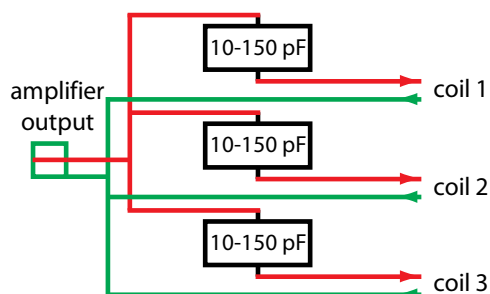


Figure 3.3 Layout of circuit designed to match three separate frequencies using a capacitor to cancel reactance on each line.

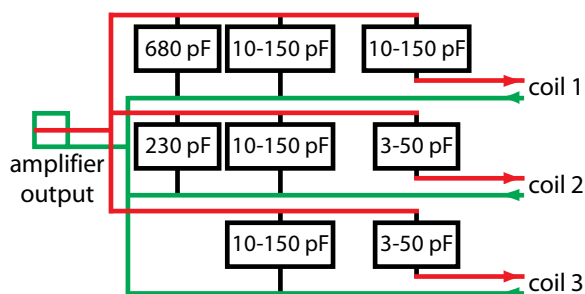


Figure 3.4 Layout of circuit designed to match three separate frequencies using an L-section at the beginning of each line.

The function generator was set to sweep from 4 MHz to 24 MHz at a rate of 100 Hz with no pause between sweeps. The amplitude was set at 50 mV peak to peak with the amplifier initially set at 50%. A line from the TTL output on the signal generator was connected to the external trigger on the oscilloscope. A Tektronix multi-channel oscilloscope was used. The oscilloscope time scale was set to display only one complete sweep on the screen. In this way it was easy to see how magnetic field magnitude varied with signal frequency. The large pickup loop was connected to Input 1 and the small pickup loop was connected to Input 2 so that both could be viewed simultaneously for comparison. Both impedance matching methods yielded similarly unanticipated results.

Method A resulted in as many as five or six separate resonant frequencies, depending on the settings of the three capacitors (Figure 3.5). Adjusting the capacitor values shifted the resonance peaks, but not as expected. Computer models predicted three peaks, each resulting from one of the capacitors. In reality, multiple resonant frequencies result from an interaction of all three capacitors so that changing any one capacitor possibly shifts the position of each of the peaks. This interdependence makes precise tuning practically impossible. Through repeated tuning attempts, the multiple peaks were resolved into three distinct resonances, though not at the desired frequencies (Figure 3.6).

Method B exhibited the same behavior as Method A, with seven or eight different resonance peaks. These were successfully resolved into four peaks, with three at roughly the desired frequencies (Figure 3.7). Tuning was even harder than with Method A since there were six variable capacitors to adjust. Neither method was particularly sensitive to whether or not the wires went through the sample rod. Nor did either method demonstrate much improvement over the unmatched coils at the desired frequencies (Figure 3.8).

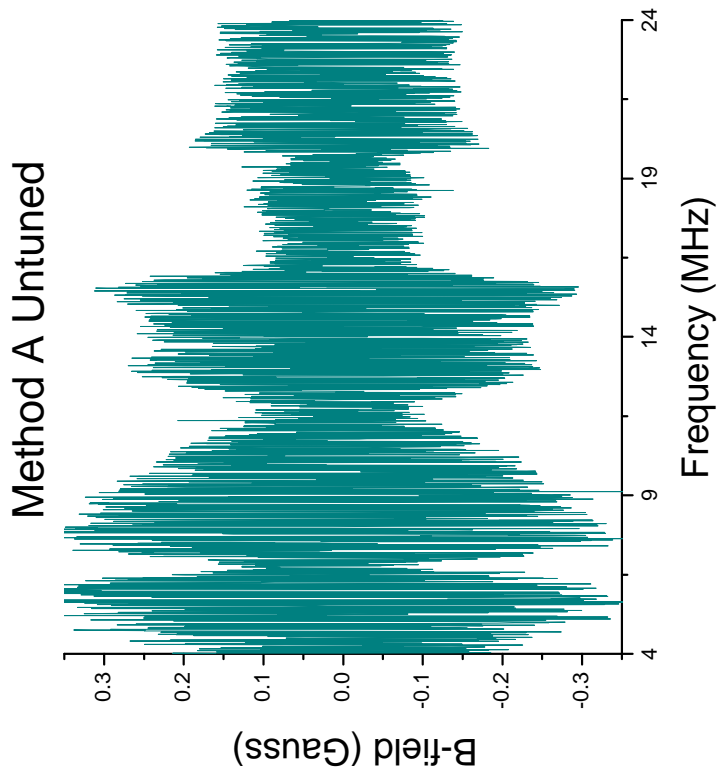


Figure 3.5 Magnetic field produced by a three-coil system on parallel wire transmission lines with an untuned series capacitor on each line; measured with the large pickup loop.

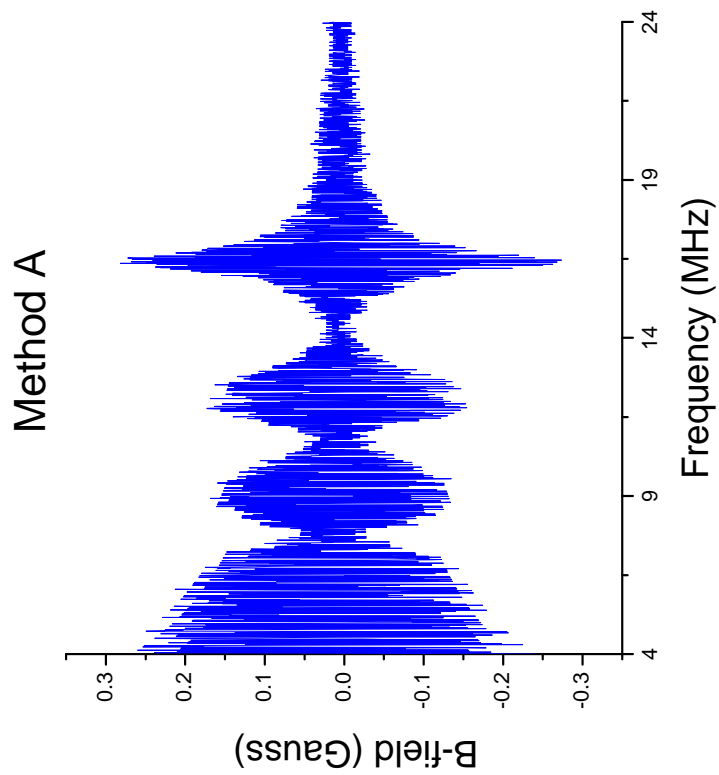


Figure 3.6 Magnetic field produced by a three-coil system on parallel wire transmission lines with a tuned series capacitor on each line; measured with the large pickup loop.

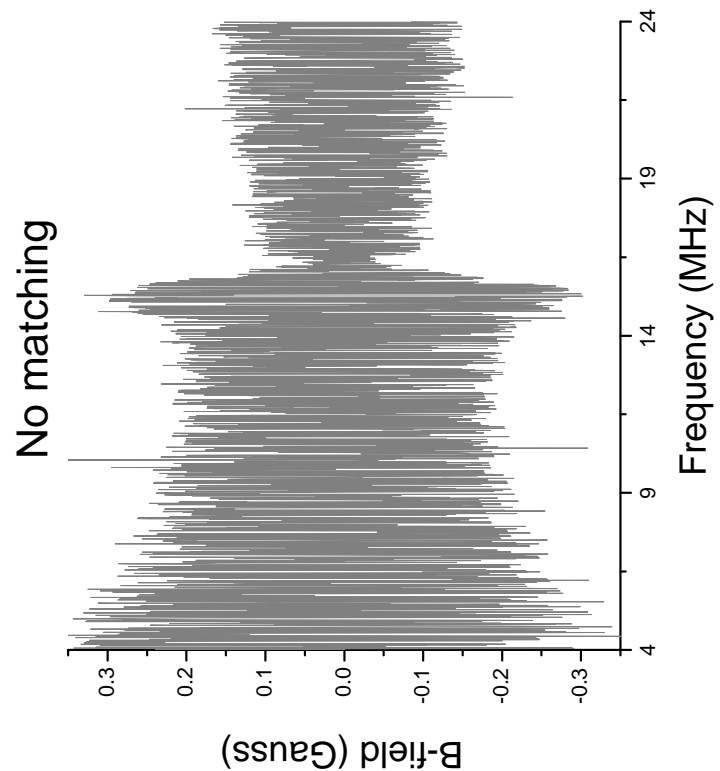


Figure 3.7 Magnetic field produced by a three-coil system on parallel wire transmission lines with a carefully tuned L-section on each line; measured with the large pickup loop.

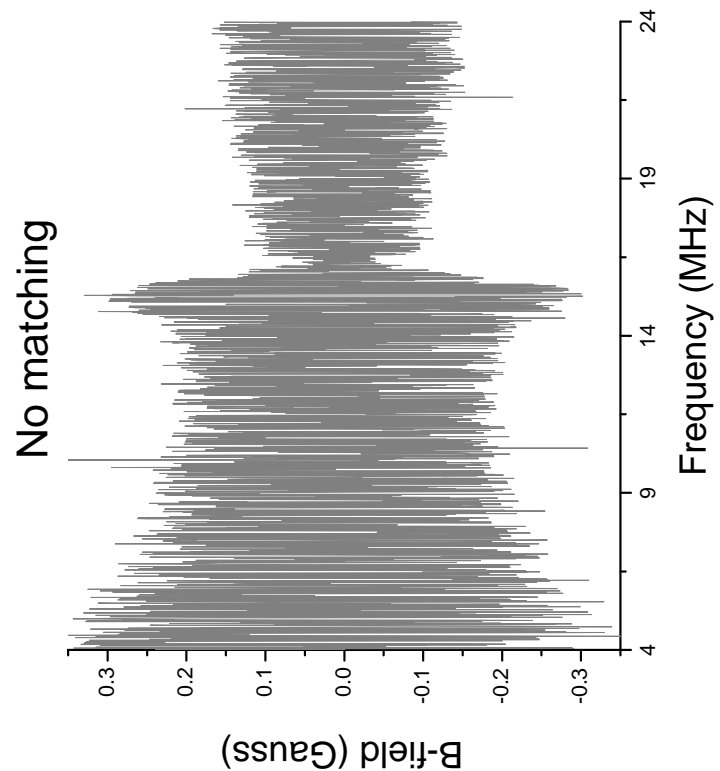


Figure 3.8 Magnetic field produced by a three-coil system on parallel wire transmission line—no impedance matching; measured with the large pickup loop.

The above plots were all obtained with the function generator signal set at 50 mV peak to peak and the amplifier set at 50%.

It was noted during experiments that placing a hand or other object on top of the amplifier or oscilloscope affected the signal. Typically the result was the flattening of one or more of the peaks. Placing a hand near one of the parallel-plate capacitors also altered the peaks, sometimes shifting them slightly. Changing the separation distance between parallel wires had little effect. Grounding the sample rod while the wires were running through it caused peak positions to shift by 1 or 2 MHz at the most.

3.4 Analysis and Recommendation

The disagreement between theory and experiment is discouraging but not at all inexplicable. Possible sources of error are obvious. Estimations of parallel wire capacitance and inductance relied on wire separation distance, which was not nearly uniform. Wire resistance was neglected. Effects of each set of parallel wires on the other two sets were neglected. Capacitors were also doubtless affected by their close proximity to each other. Coil resistance and impedance estimates may have been incorrect at higher frequencies. Mutual inductance on each coil from the other two was ignored. With all of these discrepancies it is somewhat remarkable that impedance matching was at all successful. One notable, albeit possibly coincidental, success of the computer models was the prediction that Method A would be more effective than Method B at higher frequencies. Theory also provided the correct capacitor values to create circuit resonances in the desired range.

Given the difficulty in tuning the resonant peaks and the negligible benefit over an unmatched circuit, neither impedance matching method can be recommended as a solution to the NMR problem. However, the potential of impedance matching should not

be dismissed. The mutual inductance between coils is likely the major source of error. If it can be reduced then impedance matching may be more successful. Further tests should be conducted using three separate coils each driven by a separate function generator around one of the resonant frequencies. Either Method A or Method B could be used on each line. Method A is recommended because it is easier to tune.

Bibliography

- [1] D. DiVincenzo, “The physical implementation of quantum computation,” *Fortsch. Phys.* **48** (9-11) 771-783 (2000).
- [2] J. Clarke and F. Wilhelm, “Superconducting quantum bits,” *Nature* **453** (7198) 1031-42 (2008).
- [3] M. Paris, “Optical qubit by conditional interferometry.” *Phys. Rev. A.* **62** 033813 (2000).
- [4] B. Kane, “A silicon-based nuclear spin quantum computer.” *Nature* **393** (6681) 133-37 (1998).
- [5] D. Awschalom, R. Epstein, and R. Hanson, “The diamond age of spintronics.” *Sci. Am.* **297** (4) 84-91 (2007).
- [6] D. Loss and D. DiVincenzo, “Quantum computation with quantum dots.” *Phys. Rev. A.* **57** (1) 120-26 (1998).
- [7] J. Colton, et. al., “Dependence of optically oriented and detected electron spin resonance on donor concentration in *n*-GaAs.” *Solid State Comm.* **132**, 613-16 (2004).
- [8] J. Colton, et. al., “Microsecond spin-flip times in n-GaAs measured by time-resolved polarization of photoluminescence.” *Phys. Rev. B.* **69**, 121307 (2004).

- [9] M. Mikkelsen, et. al., “Optically detected coherent spin dynamics of a single electron in a quantum dot.” *Nature Phys.* **3**, 770-73 (2007).
- [10] R. Blume, “Electron spin relaxation times in sodium-ammonia solutions.” *Phys. Rev.* **109**, 1867-73 (1958).
- [11] K. Edamatsu, “Swift control of a single spin.” *Nature* **456** (7219) 182-83 (2008).
- [12] J. Colton (private communication).
- [13] D.M. Pozar, *Microwave Engineering*, 3rd ed. (Wiley, New York, 2004), pp. 51-60.
- [14] D.M. Pozar, *Microwave Engineering*, 3rd ed. (Wiley, New York, 2004), pp. 223-27.

Appendix A

Unmatched transmission line model

The MATLAB code contained in this section was used to predict the current through the coil at the end of an unmatched transmission line, resulting in Figure 2.4. This model uses coaxial cable transmission line with two different load conditions, described in Table 2.1.

See Appendix B for a model that uses parallel wire transmission line.

```
% nomatching.m
% Written by Daniel N. Jenson
% Modified 10 November 2008
% Produces a plot of current at the end of coaxial cable transmission
% line with two different load conditions

clear;close all;clc;

% Frequency range
fmin = 4e6;
fmax = 24e6;
f = 10.^(log10(fmin):.0001:log10(fmax));
w = 2.*pi.*f;

% Source parameters
zg = 50;
% generator impedance
vg = 1;
% generator voltage

% Transmission line parameters (coaxial cable)
z0 = 40;
% characteristic impedance of transmission line
```

```

l = 1.5;
% length of transmission line in meters (coax going down sample rod)
ct = 174e-12;
% capacitance per meter of transmission line
b = w.*z0.*ct;
% definition of beta given below Eq. 9

% Coil parameters (extrapolated from data during previous run of
% experiments)
rc = .916 + 7.46559e-6.*f;
% frequency dependent resistance
lc = 15e-6;
% inductance of coil
z1 = rc + j.*lc.*w;
% complex impedance of coil (frequency dependent)

% Effective impedance of coil and coax together
zin = z0.*(z1 + j.*z0.*tan(l.*b))./(z0 + j.*z1.*tan(l.*b));
% Eq. 11

% Reflection coefficient from coax to coil
gamma = (z1 - z0)./(z1 + z0);
% Eq. 8

% Voltage at start of coax
vstart = vg.*zin./(zg + zin);
% numerator of Eq. 10

% Voltage towards coil on coax
vp = vstart./(exp(j.*l.*b) + gamma.*exp(-j.*l.*b));
% Eq. 10

% Current at end of coax (also current through coil)
I1 = (vp./z0).*(1 - gamma);
% modified form of Eq. 9 at z = 0

% Coil parameters (measured inside shell with LCR meter)
rc = .38 + 7.65e-7.*f;
% frequency dependent resistance
lc = 1.2e-6;
% inductance of coil
z1 = rc + j.*lc.*w;
% complex impedance of coil (frequency dependent)

% Effective impedance of coil and coax together
zin = z0.*(z1 + j.*z0.*tan(l.*b))./(z0 + j.*z1.*tan(l.*b));
% Eq. 11

% Reflection coefficient from coax to coil
gamma = (z1 - z0)./(z1 + z0);
% Eq. 8

% Voltage at start of coax
vstart = vg.*zin./(zg + zin);
% numerator of Eq. 10

```

```
% Voltage towards coil on coax
vp = vstart./(exp(j.*l.*b) + gamma.*exp(-j.*l.*b));
% Eq. 10

% Current at end of coax (also current through coil)
I2 = (vp./z0).*(1 - gamma);
% modified form of Eq. 9 at z = 0

% Plots
plot(f/1e6,abs(I1)*1000,'r')
hold on
plot(f/1e6,abs(I2)*1000,'m')
t = sprintf('Current through coil with %gV generator voltage',vg);
legend('Coil 1','Coil 2')
xlabel('Frequency (MHz)')
ylabel('Current (mA)')
title(t)
hold off

% end of nomatching.m
% written for MATLAB Version 7.1.0.124 (R14) Service Pack 3
```


Appendix B

Matched transmission line model

The MATLAB code contained in this section was used to predict the current through the coil at the end of a transmission line using two different types of impedance matching.

The code also generates the inductor or capacitor values required to match the amplifier to the load at a chosen frequency. These values are printed in the MATLAB command window when the code is executed. The impedance matching techniques are described briefly in section 2.3. Equations used in this code are taken from [13] and [14].

```
% current_comparison.m
% Written by Daniel N. Jenson
% Modified 15 December 2008
% Produces a plot of current at the end of parallel wire transmission
% line with two different types of impedance matching
% Also returns the inductor or capacitor values and placement required
% for each impedance matching method

clear;close all;clc;

% Frequency range
fmin = 4e6;
fmax = 24e6;
f = 10.^(log10(fmin):.0001:log10(fmax));
w = 2.*pi.*f;

% Coil parameters
rc = .38 + 7.65e-7.*f;
% frequency dependent resistance
```

```

lc = 1.2e-6;
% measured impedance
zl = rc + j.*lc.*w;
% complex impedance of coil

% Source parameters
zg = 50;
% amplifier output impedance
vg = 1;
% amplifier voltage

% Transmission line parameters (parallel wire)
l = 1.5;
% length of transmission line in meters
ct = 8.802e-12;
% capacitance per meter of transmission line
lt = 1.264e-6;
% inductance per meter of transmission line
b = sqrt(lt.*ct).*w;
% Pozar Eq. 2.12a
z0 = sqrt(lt/ct);
% Pozar Eq. 2.13

% Effective impedance of coil and transmission line together
zin = z0.*(zl + j.*z0.*tan(l.*b))./(z0 + j.*zl.*tan(l.*b));
% Pozar Eq. 2.44

% Reflection coefficient from transmission line to coil
gamma = (zl - z0)./(zl + z0);
% Pozar Eq. 2.35

% Frequency to match
f0 = 14e6;
[err,idx] = min(abs(f - f0));
w0 = w(idx);
rc0 = rc(idx);
zl0 = zl(idx);
b0 = b(idx);
zin0 = zin(idx);

% Current at coil without any matching

% Voltage at start of transmission line
vstart = vg.*zin./(zg + zin);
% taken from part of Pozar Eq. 2.70

% Voltage towards coil on transmission line
vp = vstart./(exp(j.*l.*b) + gamma.*exp(-j.*l.*b));
% Pozar Eq. 2.36a

% Current at end of transmission line (also current through coil)
Inomatch = (vp./z0).*(1 - gamma);
% Pozar Eq. 2.36b at z = 0

```

```

% Current at coil with a single element to cancel reactance
% Adapted from a script provided by Karl Warnick.

% Inductor or capacitor value required to match coil and transmission
line reactance
xm = imag(zin0);

fprintf(' To cancel reactance: \n \n')

if xm < 0
    lm = -xm/w0;
    zm = j.*lm.*w;
    fprintf(' Component should be inductor of value %g henries',lm);
else
    cm = 1/w0/xm;
    zm = -j./w./cm;
    fprintf(' Component should be capacitor of value %g farads',cm);

end

% Impedance of coil, transmission line, and matching element
ztot = zin + zm;

% Voltage and current outside of source
vout = vg.*ztot./(zg + ztot);
% taken from part of Pozar Eq. 2.70

% Voltage at start of transmission line
vstart = vout.*(1 - zm./ztot);

% Voltage towards coil on transmission line
vp = vstart./(exp(j.*l.*b) + gamma.*exp(-j.*l.*b));
% Pozar Eq. 2.36a

% Current at end of transmission line (also current through coil)
Isingleelement = (vp./z0).*(1 - gamma);
% Pozar Eq. 2.36b at z = 0

fprintf('\n \n \n');

% Current at coil with L-section matching at top of transmission line

fprintf(' For L-section matching: \n \n')

r10 = real(zin0);
% real part of load impedance at matching frequency
x10 = imag(zin0);
% imaginary part of load impedance at matching frequency

% L-section matching equations and adjusted impedance
if r10 > zg      % Situation in Pozar Figure 5.2a

    B = (x10 + sqrt(r10/zg)*sqrt(r10^2 + x10^2 - zg*r10))/(r10^2 +
x10^2); % Pozar Eq. 5.3a

```

```

    X = 1/B + xl0*zg/rl0 - zg/(B*rl0);
% Pozar Eq. 5.3b

fprintf(' RL > Zg so series element should be closer to source (Pozar
Figure 5.2a)\n')

if B < 0
    Lb = -1/(w0*B);
    fprintf(' Shunt component should be inductor of %g henries\n',Lb)
    shuntreactance = w.*Lb;
else
    Cb = B/w0;
    fprintf(' Shunt component should be capacitor of %g farads\n',Cb)
    shuntreactance = -1./(w.*Cb);
end
if X > 0
    Lx = X/w0;
    fprintf(' Series component should be inductor of %g henries\n',Lx)
    seriesreactance = w.*Lx;
else
    Cx = -1/(w0*X);
    fprintf(' Series component should be capacitor of %g farads\n',Cx)
    seriesreactance = -1./(w.*Cx);
end

    ztot = j.*seriesreactance + 1./(1./(j.*shuntreactance) + 1./zin);
% Pozar Eq. 5.1
else % Situation in Pozar Figure 5.2b

    B = sqrt((zg - rl0)/rl0)/zg;
% Pozar Eq. 5.6b
    X = sqrt(rl0*(zg - rl0)) - xl0;
% Pozar Eq. 5.6a

fprintf(' RL < Zg so shunt element should be closer to source (Pozar
Figure 5.2b)\n')

if B < 0
    Lb = -1/(w0*B);
    fprintf(' Shunt component should be inductor of %g henries\n',Lb)
    shuntreactance = w.*Lb;
else
    Cb = B/w0;
    fprintf(' Shunt component should be capacitor of %g farads\n',Cb)
    shuntreactance = -1./(w.*Cb);
end
if X > 0
    Lx = X/w0;
    fprintf(' Series component should be inductor of %g henries\n',Lx)
    seriesreactance = w.*Lx;
else
    Cx = -1/(w0*X);
    fprintf(' Series component should be capacitor of %g farads\n',Cx)
    seriesreactance = -1./(w.*Cx);
end
end

```

```

    ztot = 1./(1./(j.*shuntreactance) + 1./(j.*seriesreactance + zin));
% Pozar Eq. 5.4 inverted
end

% Voltage and current outside source
vtot = vg.*ztot./(ztot + zg);
% taken from part of Pozar Eq. 2.70
itot = vtot./ztot;
% V = I*Z

if rl0 > zg      % Situation in Pozar Figure 5.2a

% Voltage at start of transmission line (z = -l)
    vstart = vtot - j.*seriesreactance.*itot;
% voltage change across element X

else            % Situation in Pozar Figure 5.2b

% Current drawn through series element of L-section (top branch)
    itop = vtot./(j.*seriesreactance + zin);
% V = I*Z

% Voltage at start of transmission line (z = -l)
    vstart = vtot - j.*seriesreactance.*itop;
% voltage change across element X

end

% Voltage towards coil on transmission line
    vp = vstart./(exp(j.*l.*b) + gamma.*exp(-j.*l.*b));
% Pozar Eq. 2.36a at z(-l) = vstart

% Current going through coil
    ItopLsection = (vp./z0).*(1 - gamma);
% Pozar Eq. 2.36b at z = 0

fprintf(' \n')

% Plots
plot(f/1e6,abs(Inomatch)*1000,'k')
hold on
plot(f/1e6,abs(Isingleelement)*1000,'r')
plot(f/1e6,abs(ItopLsection)*1000,'b')
t = sprintf('Current through coil with %gV input',vg);
legend('no matching','single element match','L-section match')
xlabel('Frequency (MHz)')
ylabel('Current (mA)')
title(t,'fontsize',10)
hold off

% end of current_comparison.m
% written for MATLAB Version 7.1.0.124 (R14) Service Pack 3

```


Appendix C

Three-coil model

The following Maple code is used to compare impedance matching methods A and B in a three-coil configuration. Each coil is matched to a separate frequency, disregarding any interaction between coils. Each coil with its transmission line and matching elements forms a separate "leg" of the circuit. The impedances of each leg are added in parallel to find the total impedance seen by the amplifier. The total impedance determines the amplifier's power output. Once the power output is known, the voltage at the beginning of each leg is also known. From that point the current in each coil can be found separately using Ohm's Law and the equations in section 2.2.

The first block defines values common to both methods.

```

> restart:
> Zin:=Z0*(ZL+I*Z0*tan(beta*l))/(Z0+I*ZL*tan(beta*l)):
> Gamma:=(ZL - Z0)/(ZL + Z0):
> ZL:=(.38 + 7.65e-7*f)+I*(1.2e-6*w):
> f1:=9e6:
   f2:=14e6:
   f3:=19e6:
   Zg:=50:

```

```

Vg:=1:
l:=1.5:
ct:=8.802e-12:
lt:=1.264e-6:
> beta:=sqrt(lt*ct)*w:
Z0:=sqrt(lt/ct):
w:=2*Pi*f:

```

The next block contains equations for method A, which uses a single series capacitor to cancel out the reactance of Z_{in} .

```

> Ztota:=1/(1/Z1a + 1/Z2a +1/Z3a):
> Z1a:=Zin - I/w/C1:
Z2a:=Zin - I/w/C2:
Z3a:=Zin - I/w/C3:
> Vouta:=Vg*Ztota/(Zg + Ztota):
> Vstart1a:=Vouta*(1 + I/(w*C1*Z1a)):
Vstart2a:=Vouta*(1 + I/(w*C2*Z2a)):
Vstart3a:=Vouta*(1 + I/(w*C3*Z3a)):
> Vp1a:=Vstart1a/(exp(I*l*beta) + Gamma*exp(-I*l*beta)):
Vp2a:=Vstart2a/(exp(I*l*beta) + Gamma*exp(-I*l*beta)):
Vp3a:=Vstart3a/(exp(I*l*beta) + Gamma*exp(-I*l*beta)):
> I1a:=(Vp1a/Z0)*(1 - Gamma):
I2a:=(Vp2a/Z0)*(1 - Gamma):
I3a:=(Vp3a/Z0)*(1 - Gamma):
> Itota:=abs(I1a + I2a + I3a):
> X1a:=evalf(subs(f=f1,Im(Zin))):
X2a:=evalf(subs(f=f2,Im(Zin))):
X3a:=evalf(subs(f=f3,Im(Zin))):
C1:=evalf(1/(2*Pi*f1*X1a)):
C2:=evalf(1/(2*Pi*f2*X2a)):
C3:=evalf(1/(2*Pi*f3*X3a)):

```

The next block contains equations for method B, which uses L-section matching to match Z_{in} with Z_g . Capacitance values were generated for each frequency individually using the MATLAB code in Appendix B.

```

> Ztotb:=1/(1/Z1b + 1/Z2b +1/Z3b):
> Z1b:=1/(1/(Zin+Zs1)+1/Zp1):
  Z2b:=1/(1/(Zin+Zs2)+1/Zp2):
  Z3b:=1/(1/(Zin+Zs3)+1/Zp3):
> Voutb:=Vg*Ztotb/(Zg + Ztotb):
> Vstart1b:=Voutb*(1 - Zs1/(Zin + Zs1)):
  Vstart2b:=Voutb*(1 - Zs2/(Zin + Zs2)):
  Vstart3b:=Voutb*(1 - Zs3/(Zin + Zs3)):
> Vp1b:=Vstart1b/(exp(I*1*beta) + Gamma*exp(-I*1*beta)):
  Vp2b:=Vstart2b/(exp(I*1*beta) + Gamma*exp(-I*1*beta)):
  Vp3b:=Vstart3b/(exp(I*1*beta) + Gamma*exp(-I*1*beta)):
> I1b:=(Vp1b/Z0)*(1 - Gamma):
  I2b:=(Vp2b/Z0)*(1 - Gamma):
  I3b:=(Vp3b/Z0)*(1 - Gamma):
> Itotb:=abs(I1b + I2b + I3b):
> Zs1:=-I/w/Cs1:
  Zp1:=-I/w/Cp1:
  Zs2:=-I/w/Cs2:
  Zp2:=-I/w/Cp2:
  Zs3:=-I/w/Cs3:
  Zp3:=-I/w/Cp3:
  Cs1:=1.05e-10:
  Cp1:=7.67e-10:
  Cs2:=3.76e-11:
  Cp2:=3.04e-10:
  Cs3:=1.62e-11:
  Cp3:=8.64e-11:

```

And finally, the result is plotted (resulting in Figure 2.5).

```

[> plot([Itota,Itotb],f=4e6..24e6):

```


Index

Amplifier Research, 5

Biot-Savart, 7

David DiVincenzo, 2

Electron spin lifetime
in GaAs, 4
measuring, 3
 T_1 , T_2 , T_2^* , 3

Helmholtz coil
dimensions, 8
inductance, 18
resistance, 18

IBM, 2

Impedance matching
results, 23
theory, 13

LCR meter, 17

Magnetic field
desired, 10
measured, 24
predicted, 9

NMR

unsuccessful attempts at, 5
desired frequencies, 5

Ohm's Law, 10

Oxford Instruments, 3

Pozar, 12, 14, 22

Quantum computing
advantages of, 2
architectures, 2
qubits, 1
requirements, 2

Rexolite, 4

Spectromag, 3

Tektronix
function generator, 5
oscilloscope, 23

Transmission line
coaxial cable, 12
equations, 11
parallel wire, 13, 17, 22, 26